10.2478/abm-2010-0085

Asian Biomedicine Vol. 4 No. 4 August 2010; 657-661

Brief communication (Original)

Airflow inside the nasal cavity: visualization using computational fluid dynamics

Mohammed Zubair[a], Vizy Nazira Riazuddin[a], Mohammed Zulkifly Abdullah[b], Rushdan Ismail[c], Ibrahim Lutfi Shuaib[d], Suzina Abdul Hamid[c], Kamarul Arifin Ahmad[a]

[a]School of Aerospace Engineering, [b]School of Mechanical Engineering, [c]School of Medical Sciences, [d]Advanced Medical & Dental Institute, Universiti Sains Malaysia, Malaysia

Background: It is of clinical importance to examine the nasal cavity pre-operatively on surgical treatments. However, there is no simple and easy way to measure airflow in the nasal cavity.

Objectives: Visualize the flow features inside the nasal cavity using computational fluid dynamics (CFD) method, and study the effect of different breathing rates on nasal function.

Method: A three-dimensional nasal cavity model was reconstructed based on computed tomographic images of a healthy Malaysian adult nose. Navier-Stokes and continuity equations for steady airflow were solved numerically to examine the inspiratory nasal flow.

Results: The flow resistance obtained varied from 0.026 to 0.124 Pa.s/mL at flow-rate from 7.5 L/min to 40 L/min. Flow rates by breathing had significant influence on airflow velocity and wall shear-stress in the vestibule and nasal valve region.

Conclusion: Airflow simulations based on CFD is most useful for better understanding of flow phenomenon inside the nasal cavity.

Keywords: CFD, inspiration, resistance, velocity, wall shear stress

The human nasal cavity is an important component to the respiratory system. It heats and humidifies inspired air to near body-core temperature with a full saturation, and filters the air from pollutants and toxic particles to enter the airway. The complicated structure of the nose makes it difficult to measure the flow resistance. In fact, the nasal cavity is susceptible to anatomical anomalies, especially in the complex turbinate region. For this reason, any obstruction, or deformity like paranasal sinusitis, nasal polyps or septal deviation may demand surgical corrections.

The increase in the number of revision surgeries requires careful consideration before undertaking surgery [1, 2]. It is of clinical importance to measure the nasal cavity pre-operatively for decision on surgical treatments or prediction of the outcome of surgery. However, there is no simple and easy way to make accurate measurement of airflow in the nasal cavity.

Identifying the influence of nasal structure is made difficult by small-sized airways and sensitive mucosa. Rhinomanometry and acoustic rhinometry are widely used in assessment of nasal patency [3-5]. However, these methods are subjected to some limitations. Complete reliance on these methods is not adequate.

Numerical simulation based on computational fluid dynamics (CFD) may have the most potential for improving our understanding of nasal function and dysfunction. In this study, we carried out numerical simulation to explore nasal pathophysiology. A three-dimensional (3D) nasal cavity model was reconstructed from computed tomographic images (CT) of a healthy Malaysian female. Using CFD method, we examined the effect of various breathing rates on the flow features inside the nasal cavity.

Correspondence to: Mohammed Zubair, Seri Ampangan, Engineering Campus, Nibong Tebal, Penang14300, Malaysia. E-mail: mdzubairmanipal@gmail.com

Method

The study was based on an anatomical model of the normal nasal airway obtained from a CT scan of a healthy 39-year-old Malaysian female from Universiti Sains Malaysia, Medical Campus Hospital. The scan images were segmented slice by slice with an appropriate threshold value using MIMIC (Materialise, Ann Arbor, USA). The 3D polyline data of the nasal cavity was processed in CATIA and meshed with unstructured tetrahedral elements using GAMBIT 2.3.16 (Fluent, Lebanon, USA). An optimized grid with around 500,000 elements was developed from the gradient adaptation technique.

The simulation was based on the Navier-Stokes equation for 3D flow of air. Steady state laminar and turbulent airflow simulations were modeled. The airflow was assumed to be laminar for flow-rates up to 15L/min and beyond 15L/min flow was considered turbulent, as predicted by Wen et al. [6] and Segal et al. [7]. For turbulence flow, we used the SST Greek turbulence model, a two-equation turbulence model, the suitability of which has been explored by Wen et al. [6] and Mylavarapu et al. [8]. The flow boundary conditions used were 1) the nasal wall is rigid, 2) the effect of mucus is negligibly small, and 3) no-slip condition at the airway wall. By describing mass flow inlet boundary at the nostril inlet and outflow boundary condition at the outlet, we carried out numerical simulation using the commercial CFD solver FLUENT 6.3.26 (Fluent, Lebanon, USA).

Results

The comparative description of the results obtained is summarized in **Table 1.**

Average velocities obtained at certain sections inside the nasal cavity for different flow-rates (7.5, 15, 30, and 40 L/min) are plotted in **Fig. 1.** Interestingly, the maximum velocity appears at the nasal valve, which has the narrowest cross-sectional area.

Table 1. Description of nasal flow features.

Authors	Maximal velocity at nasal valve (20 L/min)	Pressure drop (20 L/min)	Flow resistance Pa.sec/mL (inspiration)
Present study	4.18 m/sec	22.6 Pa	0.026 (7.5 L/min) 0.048 (15 L/min) 0.094 (30 L/min) 0.124 (40 L/min)
Xiong et al. [12]	4.82 m/sec	-	-
Wen et al. [7]	-	18 Pa	-
Weinhold et al. [10]	-	20 Pa	-
Garcia et al. [11])	-	-	0.039 to 0.082 (15 L/min)

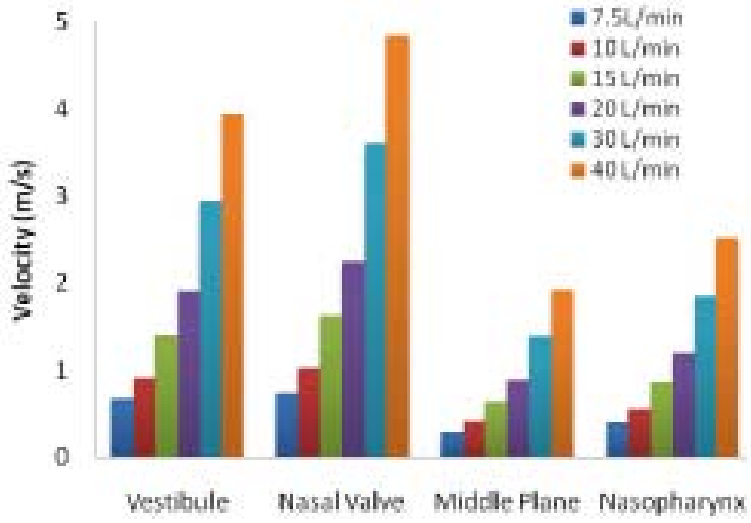

Fig. 1 Averaged velocities at different flow-rates from 7.5 to 40 L/min.

The maximum wall shear-stresses at different flow-rates (7.5, 30 and 40 L/min) are plotted in **Fig. 2**.

Figure 3 shows a family of streamline of air flow in the nasal cavity. Interestingly, re-circulatory flow appears at the olfactory region. It passes through the olfactory region, validating the previous hypothesis that flow reaching the olfactory silt is recirculatory flow.

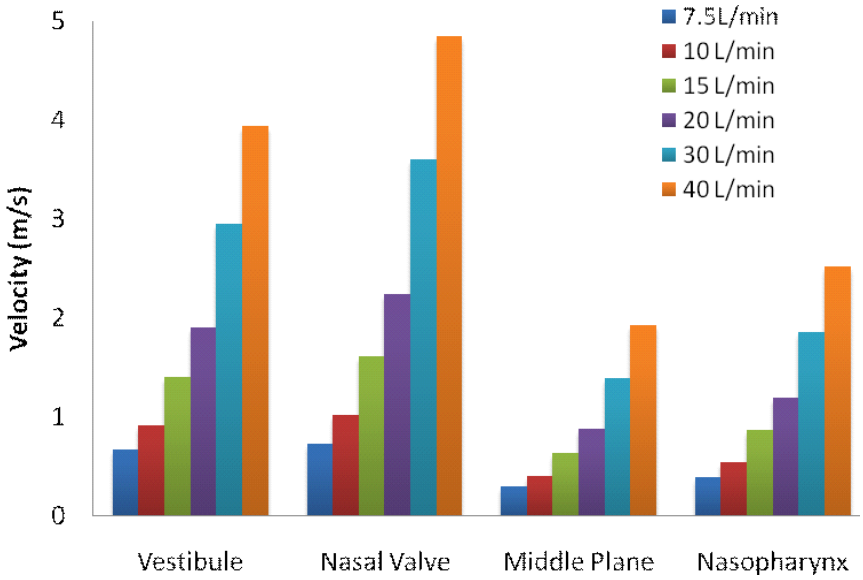

Fig. 2 Effect of different flow-rates by breathing on wall shear-stress.

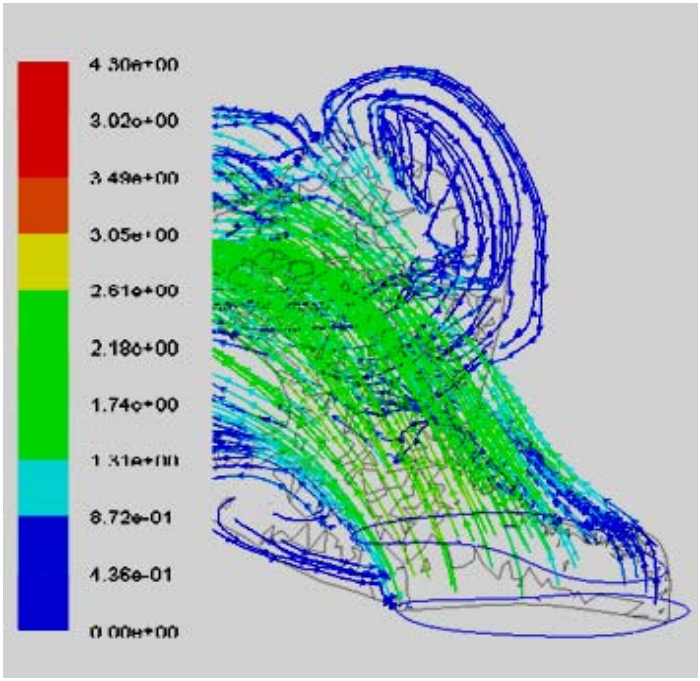

Fig. 3 A family of streamlines of air flow in the nasal cavity. Note the presence of re-circulatory flow at the olfactory region.

Discussion

Inter human differences in nasal anatomy and geometry exists. The present female nasal model was smaller in length (around 8.5 cm) in comparison to the subjects determined by Wen et al. (9.7 cm) [6] and Cheng et al. (9.5 cm) [9]. The cross-sectional area of the left nasal cavity was more than that of right cavity. The nasal valve region is located about 2.0 cm from the anterior tip of nose. This compares with the other models that are located at 3.3 cm and 2.0 cm for Wen et al. [6] and Cheng et al. [9].

The pressure drop obtained using our computational model was around 22.6 Pa for a flow-rate of 15 L/min. For the same flow rate, a pressure drop of 18 Pa and 20 Pa was observed by Wen et al. [6] and Weinhold et al. [10], respectively. The flow resistance obtained varies from 0.026 to 0.124 Pa.sec/mL for flow-rate of 7.5 L/min to 40 L/min, respectively. For a flow-rate of 15 L/min, the flow resistance obtained was around 0.048 Pa.sec/mL. Similar results were obtained by Garcia et al. [11] where the flow resistance values fell between 0.039 and 0.082 Pa-s/L for a flow-rate of 15 L/min.

According to clinical trials [13], the mean nasal resistance is around 0.145 Pa.sec/mL, which is greater than our obtained levels (0.026-0.12 Pa.sec/mL). We must note that the CFD simulations cannot be directly compared with these clinical results. The later is obtained at a transnasal pressure drop of 150 Pa, but the CFD simulation is based on resting airflow rates, where the transnasal pressure drop is considerably lower [11]. In spite of lower values obtained by CFD compared to the clinical assessments, it can be still considered reliable as a number of studies have shown the inability of the objective measurement devices like rhinomanometry to accurately measure the nasal resistance [14, 15]. The advantage with CFD is its ability to measure resistance at any locations inside the nasal cavity which are impossible to be determined using rhinomanometry or acoustic rhinometry.

In our computational model, the maximum velocity appeared at the nasal valve corresponding to the narrowest cross-sectional area (**Fig. 1**). The maximum velocity was around 4.18 m/sec for a flow-rate of 20 L/min. Its value by Xiong et al. [12] is around 4.82 m/sec. This variation may be attributed to inter human anatomical differences that exist between humans. Quantitative measurements of flow behavior at some important locations inside the nasal cavity are possible using CFD. Similar plots can be obtained for pressure and wall shear-stress.

The maximum wall shear-stress plotting shown in **Fig. 2** shows the impact of increased flow on the nasal cavity. The sneezing phenomenon, which is characterized by abrupt and very high flow-rates, results in very high value of shear-stresses at the nasal wall. This may result in injury or damage to blood vessels inside the nasal cavity. Hence, it is useful in determining the wall shear-stresses and its effect on the blood vessels.

Another important feature of the CFD simulation is its ability to visualize the flow phenomenon inside the nasal cavity (**Fig. 3**). The simulation is able to determine the re-circulatory flow regions or vortex formations within the nasal domain.

In conclusion, CFD demonstrates its usefulness in understanding the flow phenomenon inside the complicated nasal domain. It is possible to quantify and visualize the flow properties at every location within the nasal cavity. This application can further be utilized to understand the prevalence of various anomalies like septum deviation effects, turbinates, polyps, and other diseases that makes quantification difficult. It may assist the surgeon in decision making and preventing intuition-based surgeries.

Acknowledgement

The authors acknowledge the support provided through the Research University (RU) Grant No 1001/PAERO/814074 by Universiti Sains Malaysia in carrying out this work. The authors have no conflict of interest to report.

References

1. Deal T, Kountakis S. Significance of nasal polyps in chronic rhinosinusitis: symptoms and surgical outcomes. Laryngoscope. 2004; 114: 1932-5.
2. Wynn R, Har-El G. Recurrence rates after endoscopic sinus surgery for massive sinus polyposis. Laryngoscope. 2004; 114:811-3.
3. Chan KO, Huang ZH, Wang DY. Acoustic rhinometric assessment of nasal obstruction after treatment with fluticasone propionate in patients with perennial rhinitis. Auris Nasus Larynx. 2003; 30: 379-83.
4. Sipila J, Suonpaa J. A prospective study using rhinomanometry and patient clinical satisfaction to determine if objective measurements of nasal airway resistance can improve the quality of septoplasty. Eur Arch Otorhinolaryngol. 1997; 254, 387-90.

5. Ishizuka T, Ichimura K. Measurements of the nasal volume and the cross sectional areas in adult by acoustic rhinometry. Jpn J Rhinology. 1997; 36:141-4.
6. Wen J, Inthavong K, Tu J, Wang S. Numerical simulations for detailed airflow dynamics in a human nasal cavity. Respirat Physiol Neurobiol. 2008; 161: 125-35.
7. Segal RA, Kepler GM, Kimbell JS. Effects of differences in nasal anatomy on airflow distribution: a comparison of four individuals at rest. Ann Biomed Eng. 2008; 36: 1870-82.
8. Mylavarapu G, Murugappan S, Mihaescu M, Kalra M, Khosla S, Gutmark E. Validation of computational fluid dynamics methodology used for human upper airway flow simulations. J Biomech. 2009; 42:1553-9.
9. Cheng YS. Yeh HC, Guilmette RA, Simpson SQ, Cheng KH, Swift DL. Nasal deposition of ultrafine particles in human volunteers and its relationship to airway geometry. Aerosol Sci Technol. 1996; 25: 274-91.
10. Weinhold I, Mlynski G. Numerical simulation of airflow in the human nose. Eur Arch Otorhinolaryngol. 2004; 261:452-5.
11. Garcia GJM, Bailie N, Martins DA, Kimbell JS. Atrophic rhinitis: a CFD study of airconditioning in the nasal cavity. J Appl Physiol. 2007; 103:1082-92.
12. Xiong GX, Zhan JM, Jiang HY, Li JF, Rong LW, Xu G. Computational fluid dynamics simulation of airflow in the normal nasal cavity and paranasal sinuses. Am J Rhinol. 2008; 22:477-82.
13. Cole P. Nasal airflow resistance: a survey of 2500 assessments. Am J Rhinol. 1997; 11:415-20.
14. Hilberg O, Jackson AC, Swift DL, Pedersen OF. Acoustic rhinometry: evaluation of the nasal cavity by acoustic rhinometry. J Appl Physiol. 1989; 66: 295-303.
15. Austin CE, Foreman JC. Acoustic rhinometry compared with posterior rhinomanometry in the measurement of histamine- and bradykinin-induced changes in nasal airway patency. Br J Clin Pharmac. 1994; 37: 33-7.